Published OnlineFirst January 27, 2012; DOI: 10.1158/0008-5472.CAN-11-2684

Macrophage-Induced Tumor Angiogenesis Is Regulated by the TSC2–mTOR Pathway

Wei Chen[1], Tao Ma[1], Xu-ning Shen[2], Xue-feng Xia[1], Guo-dong Xu[2], Xue-li Bai[2], and Ting-bo Liang[1]

Abstract

Tumor-associated macrophages (TAM) have multifaceted roles in tumor development but they have been associated particularly closely with tumor angiogenesis. However, although the accumulation of TAM (M2 phenotype) promotes tumor angiogenesis, the mechanism through which monocytes differentiate to generate TAM is unclear. Here, we report that the mTOR pathway is a critical element in the regulation of monocyte differentiation to TAM. In human peripheral monocytes stimulated by lipopolysaccharide, mTOR was inhibited by rapamycin or activated by RNA interference–mediated knockdown of the mTOR repressor tuberous sclerosis complex 2 (TSC2). Rapamycin caused the monocytes to differentiate into M1 macrophages releasing more interleukin (IL)-12 and less IL-10, whereas TSC2 knockdown caused the monocytes to differentiate into M2 macrophages releasing less IL-12 and more IL-10. In parallel fashion, angiogenic properties were promoted or reduced in human umbilical vein endothelial cells cocultured with TSC2-deficient monocytes or rapamycin-treated monocytes, respectively. Furthermore, tumor angiogenesis and growth in murine xenografts were promoted or reduced by infusion of hosts with TSC2-deficient or TSC2-overexpressing monocytes, respectively. Finally, *in vivo* depletion of macrophages was sufficient to block the antiangiogenic effects of rapamycin on tumors. Our results define the TSC2–mTOR pathway as a key determinant in the differentiation of monocytes into M2 phenotype TAM that promote angiogenesis. *Cancer Res; 72(6); 1–10. ©2012 AACR.*

Introduction

Inflammation and cancer are connected, as cancers arise at chronic inflammatory sites (1, 2), and inflammatory cells participate in processes of tumor progression such as neoangiogenesis. Tumor-associated macrophages (TAM) play a prominent role in tumor invasion by promoting tumor angiogenesis in contrast to the antitumor effects of classical activated macrophages (3–6). Depleting macrophages in tumors reduces tumor angiogenesis (7, 8), although the molecular mechanisms governing macrophages and angiogenesis are unknown.

The mTOR is a central regulator of cell growth that phosphorylates ribosomal p70S6 kinase (p70S6K) and initiation factor 4E-binding protein 1 (4E-BP1) to control the synthesis of translation components (9). The tuberous sclerosis complex 2 (TSC2) is an upstream negative regulator of mTOR (10, 11). The TSC2–mTOR pathway may alter cytokine secretion to regulate innate immune responses, such as the monocyte macrophage system (12–14). However, the involvement of the TSC2–mTOR pathway in macrophage-induced angiogenesis is unclear.

The STAT3 controls an important inflammation-related signaling pathway in cancer development, and it is activated by tyrosine phosphorylation in both immune and tumor cells (15). STAT3 inhibits macrophage-derived antitumor immune responses (16) and is involved in macrophage differentiation and development of the tumor microenvironment (17–20). mTOR, which regulates STAT3 activation in cells including immune cells, might promote tumor angiogenesis (12, 21). Rapamycin downregulates microvessel density *in vivo* (22, 23). Together, these findings suggest that TSC2–mTOR may promote angiogenesis via macrophages and that STAT3 may be a downstream effector.

Here, we used both *in vivo* and *in vitro* assays to investigate the role of the TSC2–mTOR pathway in regulating macrophages to induce tumor angiogenesis. Our findings suggest that activating mTOR promoted macrophage-induced angiogenesis through STAT3, whereas inhibiting mTOR promoted macrophage-mediated antitumor effect.

Materials and Methods

Cell isolation and culture

Human or mouse peripheral blood mononuclear cells (PBMC) were isolated by density gradient centrifugation (12), and the monocytes were isolated from the respective

Authors' Affiliations: [1]Department of Surgery, the Second Affiliated Hospital, School of Medicine; and [2]Department of Hepatobiliary and Pancreatic Surgery, Key Laboratory of Combined Multiorgan Transplantation of Ministry of Public Health, Key Laboratory of Organ Transplantation of Zhejiang, State Key Laboratory for Diagnosis and Treatment of Infectious Disease, the First Affiliated Hospital, School of Medicine, Zhejiang University, Hangzhou, PR China

Note: Supplementary data for this article are available at Cancer Research Online (http://cancerres.aacrjournals.org/).

Corresponding Author: Ting-bo Liang, Department of Surgery, the Second Affiliated Hospital, School of Medicine, Zhejiang University, 88 Jiefang Load, Hangzhou 310003, PR China. Phone: 086-571-87315006; Fax: 086-571-87315006; E-mail: liangtingbo@zju.edu.cn

doi: 10.1158/0008-5472.CAN-11-2684

Published OnlineFirst January 27, 2012; DOI: 10.1158/0008-5472.CAN-11-2684

PBMCs by magnet-mediated cell separation (CD14 magnetic beads; Miltenyi Biotec). The phycoerythrin (PE)-conjugated antibody against CD14 was used to analyze the purity of PBMCs. The purity of human and mouse monocytes was about 95% (Supplementary Fig. S1A and S1B). The isolated monocytes were cultured in RPMI-1640 medium (Invitrogen) supplemented with 10% FBS (Invitrogen), 100 U/mL penicillin, and 100 μg/mL streptomycin. Five mice were killed for every reinfusion to have sufficient mouse monocytes.

Kupffer cells were isolated from rat livers. The nonparenchymal cells were separated with an 18% Nycodenz gradient (Nycomed Pharma A/S), and then Kupffer cells were further separated with counterflow centrifugal elutriation in a J2-MC centrifuge (Beckman-Coulter). The purity of the Kupffer cells was determined with CD68 immunofluorescence and latex bead–mediated phagocytosis (Sigma-Aldrich).

Human umbilical vein endothelial cells (HUVECs) were isolated from umbilical veins and cultured in M199 medium (Invitrogen) containing 20% FBS, 15 μg/mL endothelial cell growth supplement, 2 nmol/L L-glutamine, 100 U/mL penicillin, and 100 μg/mL streptomycin.

The Huh-7 hepatocarcinoma cell line (Japanese Collection of Research Bioresources, Sennan-shi, Osaka, Japan) was cultured similar to HUVECs. We did not conduct test and authentication for this cell line after we purchased it from the company.

Cell transfection

Monocytes were transfected with scrambled siRNA (5′ to 3′: GATCATCCTTGATCTTATA) or siRNA for TSC2 or STAT3 (Santa Cruz Biotechnology) with Lipofectamine 2000 (Invitrogen) for 48 hours before use. Mouse monocytes were similarly transfected with the TSC2 plasmid (pEGFP-c2-TSC2) or the TSC2 siRNA plasmid (pEGFP-c2-TSC2 siRNA) before being reintroduced to the mice.

Determination of cytokine concentrations

A total of 1×10^6 TSC2 siRNA-transfected human monocytes or 2×10^5 Kupffer cells were pretreated with 20 nmol/L rapamycin (Sigma-Aldrich) for 90 minutes while plated in 24-well plates and then stimulated by 100 ng/mL lipopolysaccharide (LPS; Sigma-Aldrich). After 48 hours, cell-free supernatants were collected. The concentrations of interleukin (IL)-12-p40, IL-12-p70, IL-6, TNF-α, IL-10, VEGF, IL-1, and monocyte chemotactic protein-1 (MCP-1) were measured by ELISA using kits (R&D Company).

Immunoblot analysis

A total of 1×10^7 human monocytes were stimulated as indicated after 24 hours of starvation in serum-free medium. Cellular lysates (40 μg) were analyzed by standard Western blotting techniques. Immunoreactive bands were developed by enhanced chemiluminescence (ECL; GE Healthcare) and visualized by autoradiography (Kodak). Relative levels of total and phosphorylated proteins were determined with these antibodies: anti-phospho-STAT3 (Tyr705) and anti-STAT3 (Santa Cruz Biotechnology); anti-phospho-TSC2 (Ser939), anti-TSC2, anti-phospho-mTOR (Ser2448), anti-mTOR, anti-phospho-p70S6k (Thr389), anti-p70S6K, anti-phospho-4E-BP1 (Thr37/46), anti-4E-BP1, mouse anti-phospho-NK-κB, and mouse anti-phospho-p38/MAPK (Cell Signaling); and anti-GAPDH (Shanghai Kangcheng).

Matrigel angiogenesis assay *in vitro*

A total of 2×10^4 primary HUVEC cells were plated on 24-well plates coated with Matrigel (BD Bioscience), incubated for 1 hour at 37°C with 5% CO_2, cocultured with monocytes for 12 hours, and subsequently the development of capillary structures and tubular networks was analyzed by light microscopy (Leica Microsystems).

Subcutaneous xenograft of Huh-7 cells in nude mice

Male nude mice that were 5 weeks old weighing 18 to 20 g (Shanghai Experimental Animal Institute, Shanghai, China) were housed in a pathogen-free room. The experimental animals were handled in compliance with the guidelines of the Animal Ethics Committee of Zhejiang University (Hangzhou, PR China). After Huh-7 cells were harvested, 10^6 cells were resuspended in 100 μL saline solution and inoculated into one flank of each mouse. After 3 weeks, the tumors were 100 mm^3 and the mice were divided into 3 treatment groups.

In experiment A, 35 tumor-bearing mice were divided into 4 groups: control group ($n = 5$), rapamycin group (5 mice intraperitoneally administered with 1 mg/kg rapamycin daily), $GdCl_3$ group (5 mice injected with 10 mg/kg $GdCl_3$ once a week through the caudal vein), and combined group (20 mice injected with both $GdCl_3$ and rapamycin). After 2 weeks, 5 mice from each group were killed, and then the xenografts were removed and saved for additional research. The remaining 15 mice from the combined group were injected with $GdCl_3$ again, and then divided into 3 groups: rapamycin group (5 mice administered 1 mg/kg rapamycin daily), rapamycin plus monocyte group (5 mice administered 1 mg/kg rapamycin daily and daily infusion of 5×10^6 mouse monocytes), and monocyte groups (5 mice had only 5×10^6 mouse monocytes reintroduced the next day). Injected monocytes were not pretreated with rapamycin or LPS. The different experimental monocytes were directly injected intravenously into mice. After 1 week, the mice were sacrificed by cervical dislocation, and the xenografts were removed for analysis.

In experiment B, 20 male nude mice were treated with subcutaneous xenografts of Huh-7 cells established as earlier and divided into 4 groups: control group (5 mice injected with vehicle daily), $GdCl_3$ group (5 mice injected with 10 mg/kg $GdCl_3$ weekly), TSC2 siRNA group (5 mice treated with 5×10^6 monocytes transfected with the TSC2 siRNA), and TSC2 group (5 mice treated with 5×10^6 monocytes transfected with the TSC2).

In experiment C, 20 additional tumor-bearing nude mice were divided into 4 groups: control group (5 mice injected with vehicle daily), NSC 74859 group [5 mice treated with 5 mg/kg NSC 74859 (Merck KGaA) intraperitoneally every other day], $GdCl_3$ group (5 mice injected with 10 mg/kg $GdCl_3$ weekly), and combined group (5 mice injected with both 10 mg/kg $GdCl_3$ and 5 mg/kg NSC 74859 as described earlier). All the mice were killed by cervical dislocation 2 weeks later. The xenografts were removed and stored for further examination.

Published OnlineFirst January 27, 2012; DOI: 10.1158/0008-5472.CAN-11-2684

Rat tumor induction

A total of 20 male Sprague-Dawley rats with body weights of 160 to 180 g and aged from 6 to 7 weeks (Shanghai Experimental Animal Institute, Shanghai, China) had hepatomas induced by continuously administering 0.01% diethylnitrosamine via drinking water for 12 weeks.

Two weeks after tumor inoculation, the 10 rats in the rapamycin and 10 in the control group had 2 mg/kg rapamycin (Hangzhou Huadong Medicine Group) or saline solution, respectively administered intragastrically. All rats were sacrificed by cervical dislocation 4 weeks later, and the livers were removed, photographed, and examined by immunohistochemistry for CD31 and CD68 expression.

Histology and immunohistochemistry

Formalin-fixed tumor sections were stained with hematoxylin and eosin. Both CD31 and CD68 were immunohistochemically examined on the paraffin sections using primary antibodies diluted 1:75 (Santa Cruz Biotechnology). The mean vessel density was quantified in sections stained for CD31 by capturing 10 random fields (0.159 mm^2) at $\times 100$ magnification.

Statistical analysis

Data are presented as mean with SD. Independent 2-sample *t* tests compared differences between 2 groups, and one-way ANOVA with the least significant difference test for *post hoc* comparisons compared differences between 3 or 4 groups. A *P*

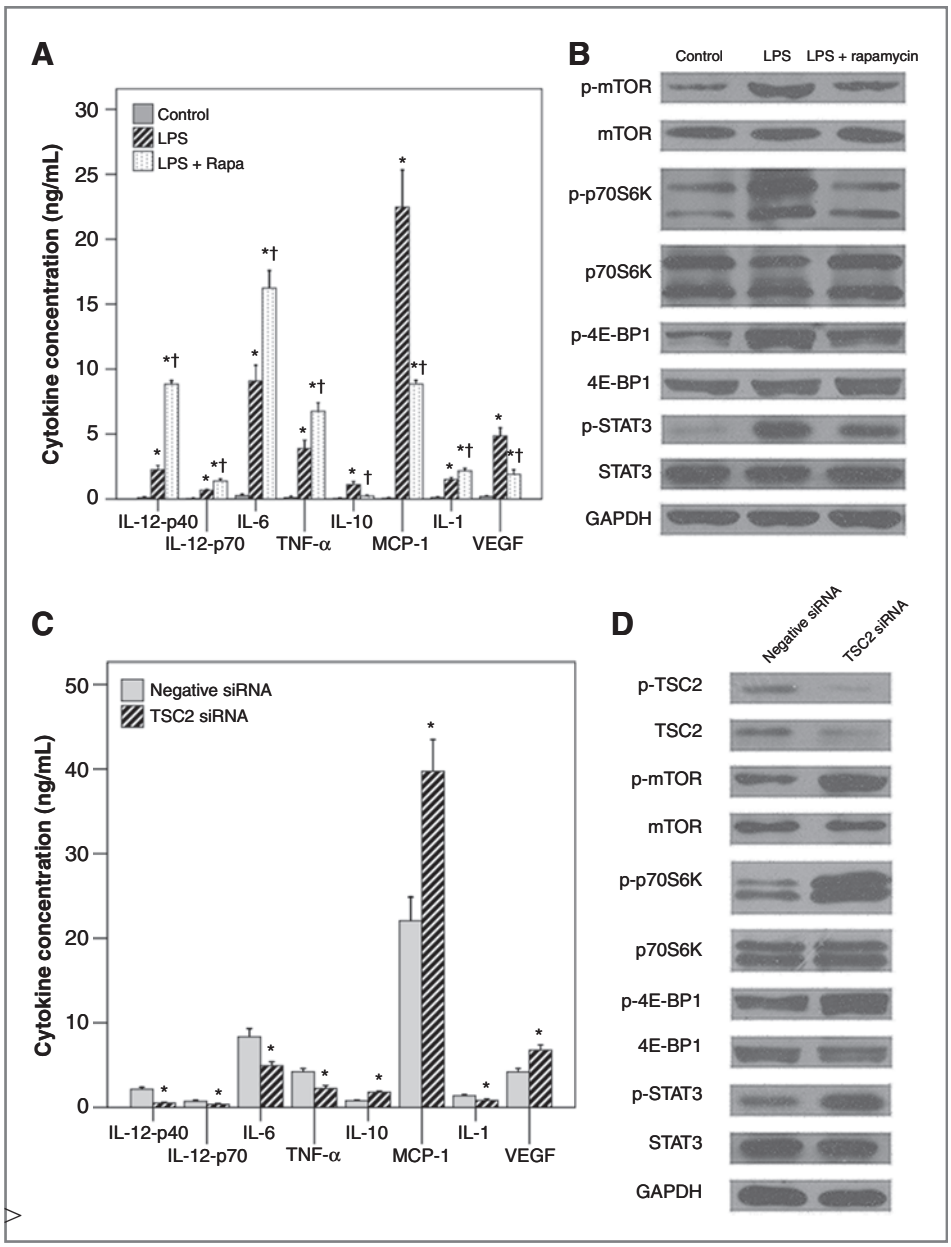

Figure 1. The TSC2–mTOR pathway regulated cytokine secretion by human monocytes. A, expression of cytokines by human monocytes which was stimulated with LPS or incubated with rapamycin (Rapa) and then stimulated with LPS by ELISA assay. Data represent the mean ± SD. *, significant difference compared with the control group; †, significant difference compared with the LPS group. B, the effects of LPS stimulation and rapamycin treatment on the intracellular mTOR pathway were analyzed by Western blotting. C, expression of cytokines by human monocytes which stimulated with TSC2 siRNA by ELISA. Data represent the mean ± SD. *, significant difference compared with negative siRNA group. D, Western blotting analyzed the changes in the proteins of the intracellular mTOR pathway after transfection with negative or TSC2 siRNA. GAPDH, glyceraldehyde-3-phosphate dehydrogenase.

Published OnlineFirst January 27, 2012; DOI: 10.1158/0008-5472.CAN-11-2684

value below 0.05 indicated statistical significance. Statistics were analyzed with SPSS 15.0 software (SPSS Inc.).

Results

Manipulating the TSC2–mTOR pathway modulated cytokine secretion and vessel formation

To investigate the impact of mTOR activity on macrophages, cytokine secretion was assessed in human monocytes (Fig. 1). Monocytes in rapamycin + LPS group secreted more IL-12-p40, IL-12-p70, IL-6, TNF-α, and IL-1 and secreted significantly less IL-10, MCP-1, and VEGF than in the LPS group (All $P < 0.05$; Fig. 1A) and the majority of cells in the population shifted to expressing IL-12-p40 (Supplementary Fig. S1C). LPS treatment significantly increased the release of these cytokines compared with non-LPS–treated control cells. Treatment with LPS increased the phosphorylation of mTOR compared with control on Ser2448 (a frequent site of mTOR phosphorylation; ref. 24), 4E-BP1, and STAT3 of the downstream mTOR pathway (Fig. 1B). Treatment with rapamycin reduced mTOR phosphorylation although the phosphorylation was higher than the untreated control. CD206 (mannose receptor), a marker of M2 macrophages, was not detected in the rapamycin + LPS treatment group (Supplementary Fig. S1D) but it was highly expressed on TSC2 siRNA–treated cell surfaces (Supplementary Fig. S1E). To assess whether rapamycin may affect the phosphorylation of other LPS-stimulated pathways, we evaluated the phosphorylation NF-κB and p38/mitogen-activated protein kinase (MAPK) after rapamycin treatment. Rapamycin did not affect the phosphorylation of p38 but did increase the phosphorylation of NF-κB (Supplementary Fig. S2A and S2B).

The effect of reduced TSC2 on cytokine secretion and protein expression was examined by transfection of cells with TSC2 siRNA. Compared with monocytes transfected with unspecific siRNA, monocytes transfected with TSC2 siRNA secreted significantly less IL12-p40, IL12-p70, IL-6, TNF-α, and IL-1 and secreted more IL-10, MCP-1, and VEGF (all $P < 0.05$; Fig. 1C). Increased phosphorylation of mTOR, p70S6K, 4E-BP1, and STAT3 was detected in monocytes transfected with TSC2 siRNA (Fig. 1D). These results suggest that monocytes treated with rapamycin and subsequently stimulated by LPS developed the M1-like macrophage phenotype, whereas monocytes transfected with TSC2 siRNA developed the M2-like macrophage phenotype.

To define the potential role of mTOR in monocyte-induced angiogenesis, vessel formation by human monocytes with different treatments was assayed *in vitro* (Fig. 2). Rapamycin treatment significantly reduced LPS-induced vessel formation ($P = 0.004$; Fig. 2A and B). Conversely, TSC2 siRNA treatment significantly increased vessel formation ($P = 0.005$; Fig. 2C and D). However, addition of VEGF antibody did not significantly block TSC2 siRNA–induced angiogenesis (see Supplementary Fig. S3A and S3B).

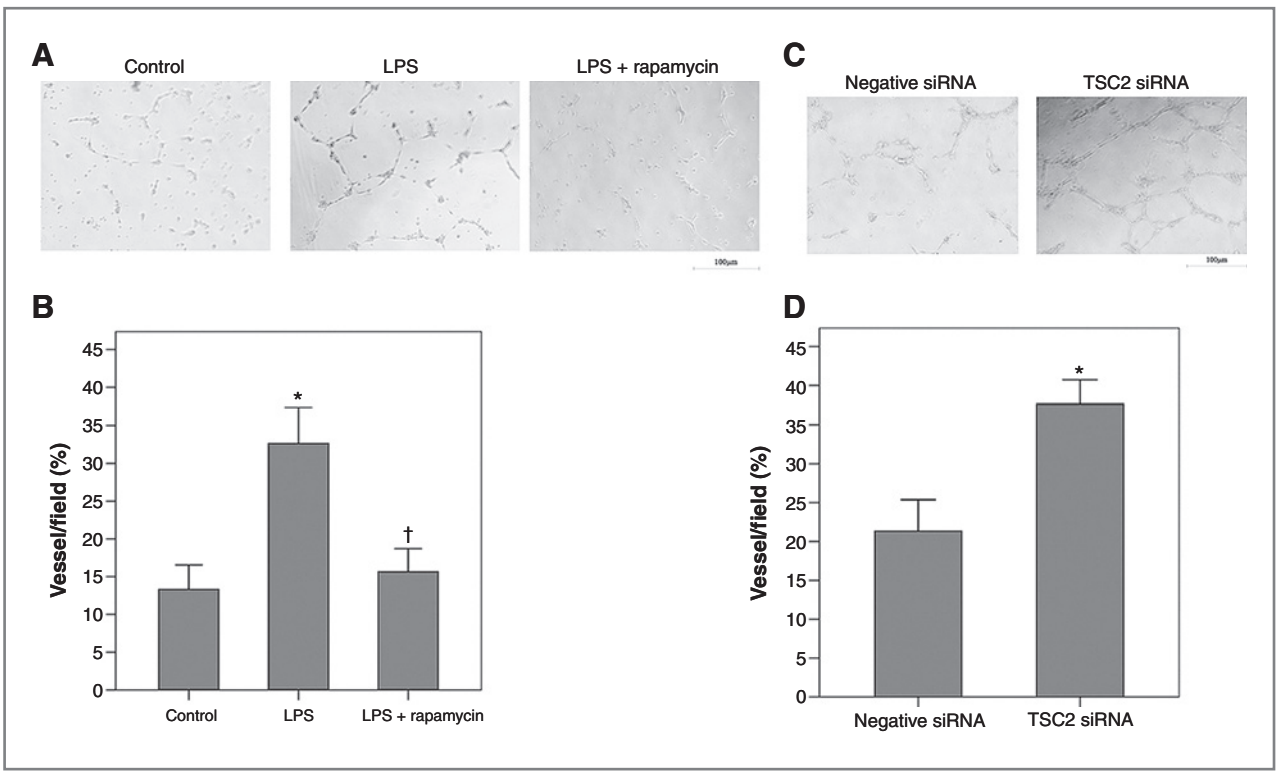

Figure 2. The TSC2–mTOR pathway regulated the formation of macrophage-induced vessels by HUVECs *in vitro*. The vessel formation of the HUVECs which were plated in 24-well plates coated with Matrigel and cocultured with human monocytes which were pretreated with LPS and/or rapamycin (A and B) or TSC2 siRNA (C and D). Data represent mean ± SD. *, a significant difference compared with the control group; †, a significant difference compared with the LPS group.

Published OnlineFirst January 27, 2012; DOI: 10.1158/0008-5472.CAN-11-2684

Macrophages mediate the antitumor effects of rapamycin *in vivo*

Because rapamycin inhibits tumor angiogenesis *in vivo*, nude mice were inoculated with Huh-7 hepatocarcinoma cells to form subcutaneous tumors and subsequently treated with $GdCl_3$ to deplete monocytes or rapamycin to inhibit mTOR, or both (Fig. 3, experiment A). The monocytes/macrophages in $GdCl_3$-treated tumor tissue were significantly lower than in the untreated group (0.17% vs. 9.4%; Supplementary Fig. S4). The $GdCl_3$-treated mice trended toward lower gross tumor volume and relative lower ratio of tumor weight to body weight (15.4 vs. 39.6 mg/g, $P = 0.0022$). Interestingly, the mice treated with both $GdCl_3$ and rapamycin had larger tumors than rapamycin alone (Fig. 3A, $P < 0.05$). The rapamycin-treated mice had the smallest tumors and a lower ratio of tumor weight to body weight (4.6 mg/g) than control mice ($P = 0.0001$, right).

The reintroduction of exogenous monocytes into $GdCl_3$-treated mice rescued tumor growth (Fig. 3B) and the addition of exogenous monocytes plus rapamycin significantly inhibited tumor growth ($P < 0.0001$). Further analysis of microvessel density found that rapamycin significantly inhibited exogenous monocyte-induced microvessel density formation (Fig. 3C). These findings suggest that rapamycin induced monocytes to differentiate into the antitumor M1 phenotypes.

TSC2–mTOR signal pathway controls angiogenesis induced by macrophages *in vivo*

In human and mouse monocytes, downregulation of TSC2 by TSC2 siRNA transfection significantly increased the ratio of phosphorylated mTOR/total mTOR in a time-dependent pattern, whereas overexpression of TSC2 by TSC2 cDNA transfection significantly decreased mTOR phosphorylation (Fig. 4A and B).

To investigate the role of mTOR in the xenograft tumor growth induced by macrophages *in vivo*, we manipulated TSC2 expression in monocytes that had been reintroduced into mice (Fig. 4C, experiment B). Mice treated with monocytes overexpressing TSC2 had the smallest tumor size. Tumors from mice treated with TSC2 siRNA monocytes were larger than mice treated with $GdCl_3$ ($P = 0.0003$) or control mice ($P < 0.05$). Microvessel density assay indicated that overexpression of TSC2 significantly inhibited exogenous monocyte-induced blood vessel formation, whereas TSC2 siRNA–treated monocytes dramatically induced angiogenesis (Fig. 4D).

STAT3 mediates the effects of rapamycin on cytokine secretion of monocytes

To elucidate the downstream target of mTOR, we investigated the effect of rapamycin on STAT3, which is required for

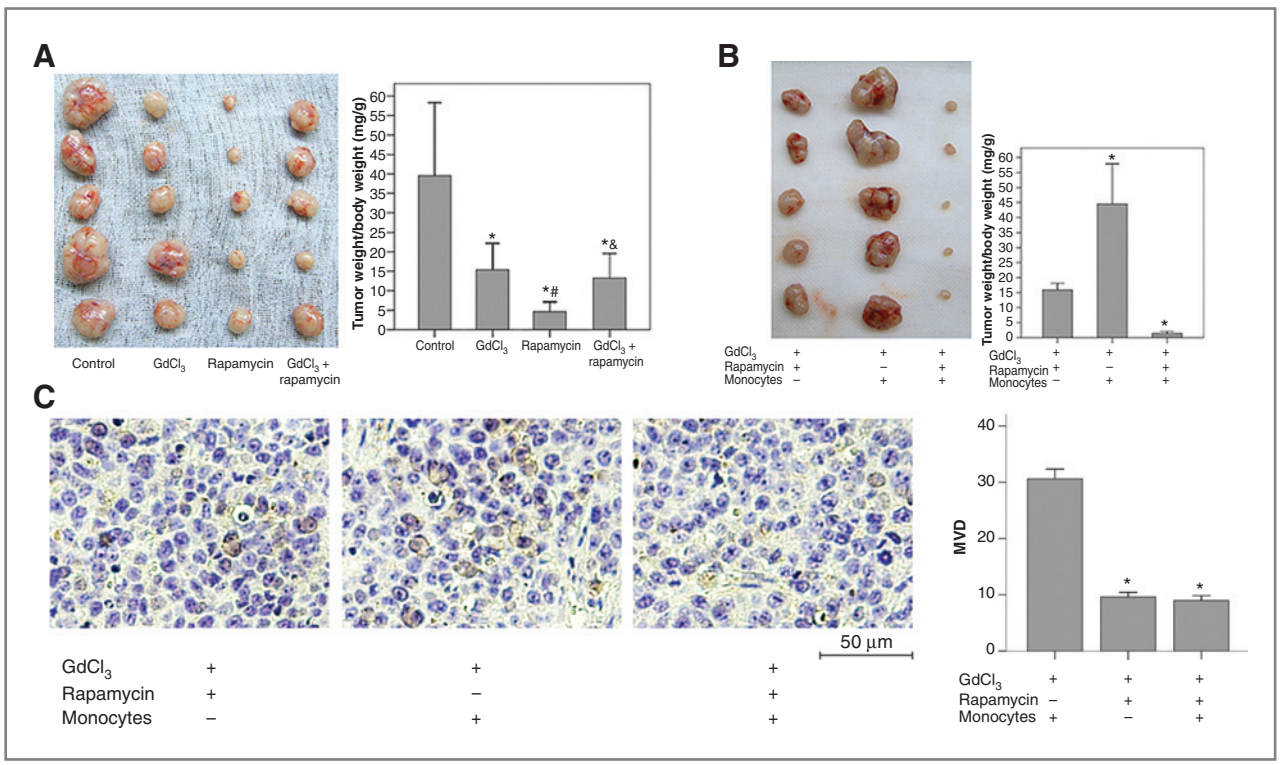

Figure 3. The macrophages mediated the antitumor effects of rapamycin *in vivo*. Nude mice were treated with rapamycin in the presence or absence of monocytes as described in experiment A in the Materials and Methods. A, their tumors were imaged (left), and the ratios of the weight of their tumors to their body weights were quantified (right). *, $P < 0.05$ in comparison to control; #, $P < 0.05$ in comparison to $GdCl_3$; &, $P < 0.05$ in comparison to rapamycin (Rapa). B, the effects of rapamycin on tumor growth with or without reintroduction of exogenous monocytes into $GdCl_3$-treated mice were detected. Their tumors, after receiving the various treatments, were imaged (left), and the ratios of the weight of their tumors to their body weights were quantified (right). *, $P < 0.05$ in comparison to the $GdCl_3$ and rapamycin group. C, the effects of rapamycin on blood vessel formation in the tumor from (B) were investigated. †, $P < 0.05$ in comparison to $GdCl_3$ and monocytes group. Data represent mean ± SD ($n = 5$). MVD, microvessel density.

Published OnlineFirst January 27, 2012; DOI: 10.1158/0008-5472.CAN-11-2684

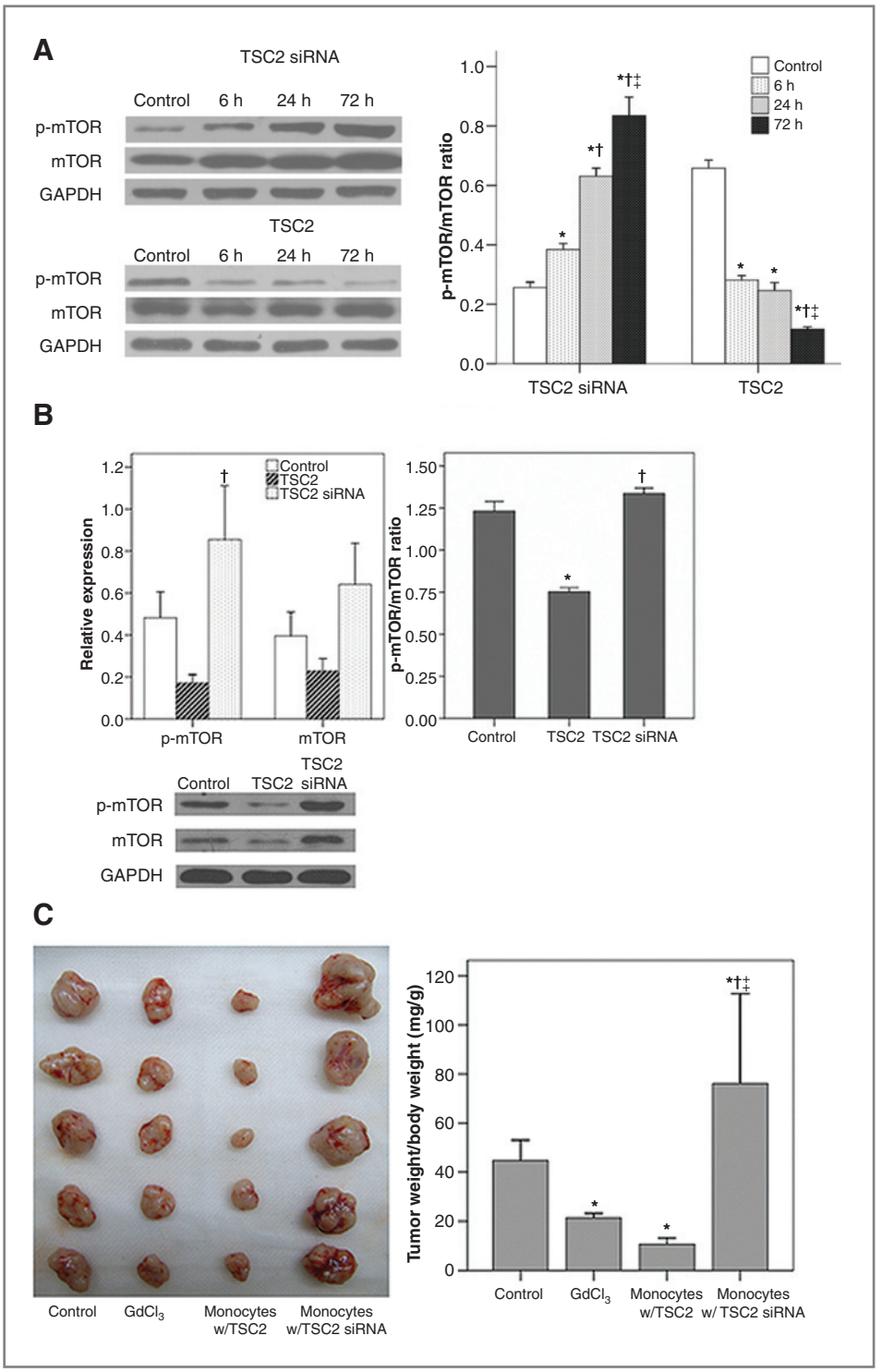

Figure 4. Effects of TSC2 on mTOR and tumor formation. A, phosphorylation of mTOR and total mTOR in human monocytes were detected after transfection with TSC2 cDNA or TSC2 siRNA for different time (6, 24, and 72 hours) *in vitro*. *, $P < 0.05$ in comparison with Control; †, $P < 0.05$ in comparison with 6 hours; ‡, $P < 0.05$ in comparison with 24 hours. B, effects of overexpression or knockdown TSC2 on phosphorylation of mTOR and total mTOR in mouse monocytes were reversed *in vitro*. Data represent 3 separate experiments. *, $P < 0.05$ in comparison to the control group; †, $P < 0.05$ in comparison to the TSC2 group. C, tumor formation in nude mice as described in experiment B in the Materials and Methods. *, $P < 0.05$ in comparison to the control group; †, $P < 0.05$ in comparison to the $GdCl_3$ group; ‡, $P < 0.05$ in comparison to the TSC2 group.

IL-10 secretion. NSC 74859 treatment or knocking down STAT3 significantly increased the concentration of IL-12-p40 and reduced the concentration of IL-10 (all $P < 0.001$; Fig. 5A). NSC 74859 inhibits STAT3 activity by inhibiting STAT3 complex formation, DNA-binding, and transcriptional activities (25). NSC 74859 treatment and STAT3 siRNA transfection decreased phosphorylation of STAT3 (Fig. 5B) and inhibited blood vessel formation (Fig. 5C). *In vivo* xenografts indicated that tumors from mice treated with NSC 74859 were smaller than those from control mice ($P < 0.0001$), but mice treated

Published OnlineFirst January 27, 2012; DOI: 10.1158/0008-5472.CAN-11-2684

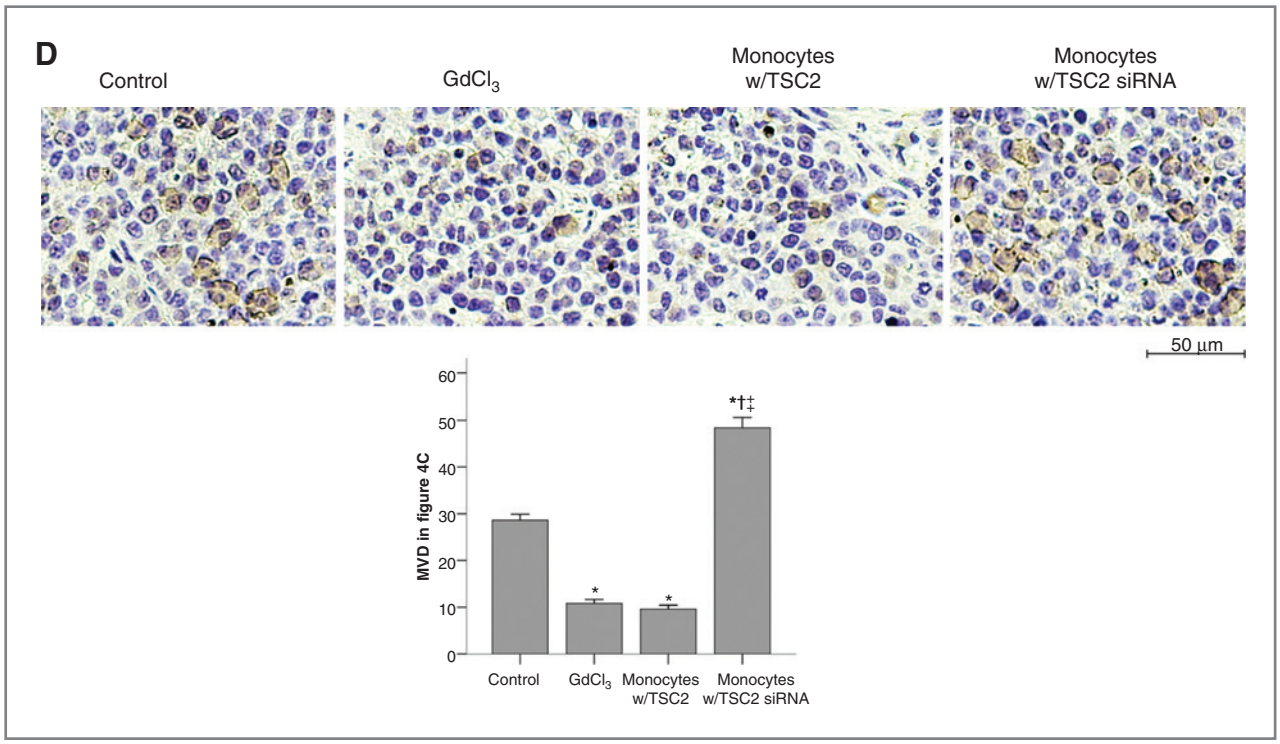

Figure 4. (*Continued*) D, the effects of TSC2 on blood vessel formation in the tumor from (C) were investigated. *, $P < 0.05$ in comparison to the control group; †, $P < 0.05$ in comparison to the $GdCl_3$ group; ‡, $P < 0.05$ in comparison to the TSC2 group. Data represent mean ± SD ($n = 5$). GAPDH, glyceraldehyde-3-phosphate dehydrogenase; MVD, microvessel density.

with $GdCl_3$ or with $GdCl_3$ and NSC 74859 had statistically similar tumor sizes (Fig. 5D, experiment C). We further found that treatment with NSC 74859 blocked TSC2 siRNA–induced blood vessel formation, indicating that STAT3 is necessary for mTOR-induced angiogenesis (Supplementary Fig. S5A and S5B).

The cytokine secretion of Kupffer cells and hepatocarcinogenesis induced by diethylnitrosamine are affected by mTOR

The Kupffer cells were identified by CD68 immunofluorescent staining (Fig. 6A). Treating the Kupffer cells with rapamycin *in vitro* increased the secretion of IL-12-p40 ($P = 0.011$), TNF-α ($P = 0.002$), and IL-6 ($P < 0.001$) and decreased IL-10 compared with control (Fig. 6B, $P = 0.002$). Furthermore, large clumps of tumor were easily seen in the liver of the control rats but not in rapamycin-treated animals (Fig. 6B). In addition, less CD31 staining was detected in the liver of rapamycin-treated rats; however, CD68 staining did not alter the number of Kupffer cells (Fig. 6C).

Discussion

In this study, we found that inhibiting of mTOR by either rapamycin or overexpression of TSC2 or blocking STAT3 in monocytes/macrophages promoted the release cytokines of the M1 and inhibited tumor growth *in vitro* and *in vivo*. These effects were confirmed with decreased tumor angiogenesis and the requirement of monocytes. We also confirmed that activating the mTOR signaling pathway by treating monocytes/macrophages with TSC2 siRNA promoted release of cytokines of the M2 phenotype and promoted tumor growth. These findings were confirmed by the increased tumor and the requirement for monocytes.

TAMs are considered a polarized population of M2 macrophages, especially when the tumor begins to invade, vascularize, and develop (3, 4). The classification of polarized macrophages as either the M1 or M2 phenotype is mainly based on differential secretion of cytokines. The M1 phenotype secretes IL-12 and TNF and later the M2 phenotype secretes IL-10. This study found that TAMs profoundly influenced the regulation of tumor angiogenesis and that depleting macrophages reduced vascular density and delayed tumor growth.

This study shows that inhibiting mTOR increased IL-12 production and decreased IL-10 production in monocytes, in agreement with previous studies (12, 13). The opposing roles of IL-12 and IL-10 provide a new explanation of the antitumor effects of inhibiting mTOR activity. The fact that IL-12-p70 was only modestly upregulated might suggest that excess IL-12-p40 may form homodimers, although we did not detect IL-12-p40 homodimers in these experiments.

Because the antitumor effects of rapamycin are mainly attributed to inhibited angiogenesis (22, 23), it is exciting that the rapamycin effects were eliminated by depleting macrophages with $GdCl_3$, a known inhibitor of Kupffer cell activation (26, 27). Reintroducing monocytes recovered the antitumor effects of rapamycin. Rapamycin enhanced and TSC2 siRNA attenuated the phagocytic capability of macrophages

Published OnlineFirst January 27, 2012; DOI: 10.1158/0008-5472.CAN-11-2684

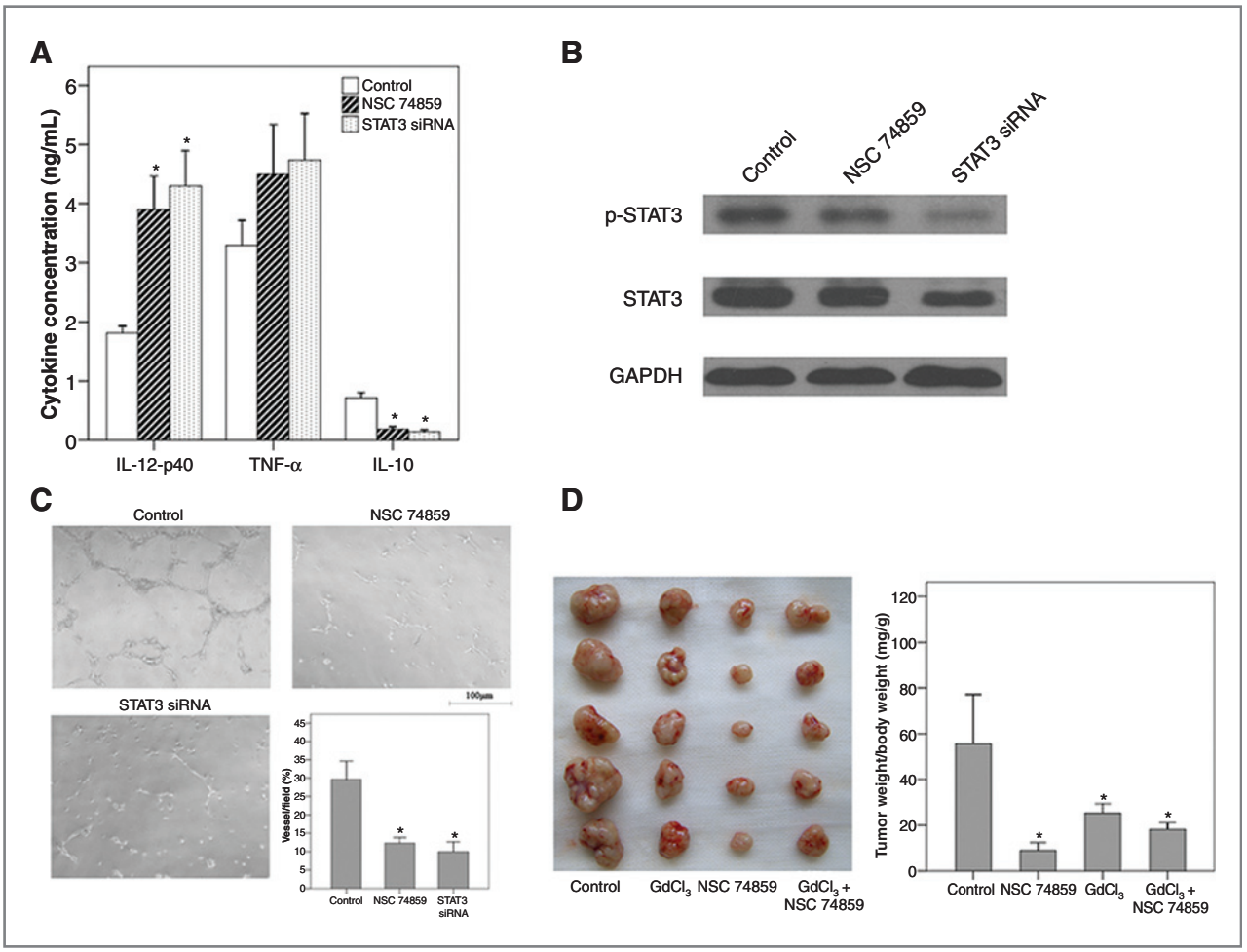

Figure 5. Inhibiting STAT3 blocked the angiogenesis induced by macrophages both *in vitro* and *in vivo* in a manner similar to rapamycin. A, the production of IL-12-p40, TNF-α, and IL-10 by monocytes with different treatments. Data represent the mean ± SD. *, a significant difference compared with the control group ($P < 0.05$). B, Western blotting analyzed the expression of STAT3 after the treatments shown in (A). C, vessel-like structure formation by HUVECs cocultured with human monocytes with different treatments in 24-well plates coated with Matrigel. *, a significant difference compared with the control group ($P < 0.05$). D, tumor formation in nude mice as described in experiment C in the Materials and Methods under STAT3 inhibitor (NSC 74859, 5 mg/kg) treatment. *, a significant difference compared with the control group ($P < 0.05$).

(Supplementary Fig. S6), which was reversed by reintroduction of macrophage infiltration into tumors (Supplementary Fig. S7A–S7C). These findings strongly suggested that the antitumor effects of rapamycin were mediated by induction of macrophages with the antitumor M1 phenotype.

Inhibiting mTOR altered the monocyte cytokines *in vitro* by increasing IL-12 and decreasing IL-10. This finding suggested that the mTOR signal may participate in polarizing macrophages, which would explain the essential role of monocytes in the ability of rapamycin to inhibit angiogenesis. Phosphorylation of mTOR at Ser2448 is mediated by the p70S6 kinase (24) and our findings suggest that this may be controlled by inhibiting the phosphorylation of p70S6. We found that rapamycin did not inhibit the phosphorylation of p38 but did enhance the phosphorylation of NF-κB. Releasing of IL-12 required activated NF-κB in macrophages (28, 29). This indicated that the cytokine released by rapamycin-treated macrophages might be mediated through NF-κB pathway. In addition, although TSC2 siRNA resulted in an upregulation of VEGF, adding of VEGF antibody did not significantly block TSC2 siRNA–induced angiogenesis.

Our findings indicated that mTOR regulates the ability of macrophages to induce angiogenesis. Rapamycin downregulates secretion of IL-10, which promotes the production of VEGF in both immune and tumor cells resulting in strengthening of the macrophage T-helper cell (T_H1) response. Our experiments suggest that that the TSC2–mTOR pathway–regulated angiogenesis may be mediated by other growth factors, not only through VEGF. We also found that rapamycin enhanced TSC2 siRNA attenuation of macrophage phagocytosis (Supplementary Fig. S6). Although our rapamycin experiments support the idea that the mTOR pathway acts via monocytes to promote tumor growth, it is possible that the effect of rapamycin may affect monocytes through other mechanism. In an *in vitro* experiment, we found that rapamycin mainly stimulated monocytes to release cytokines which

Published OnlineFirst January 27, 2012; DOI: 10.1158/0008-5472.CAN-11-2684

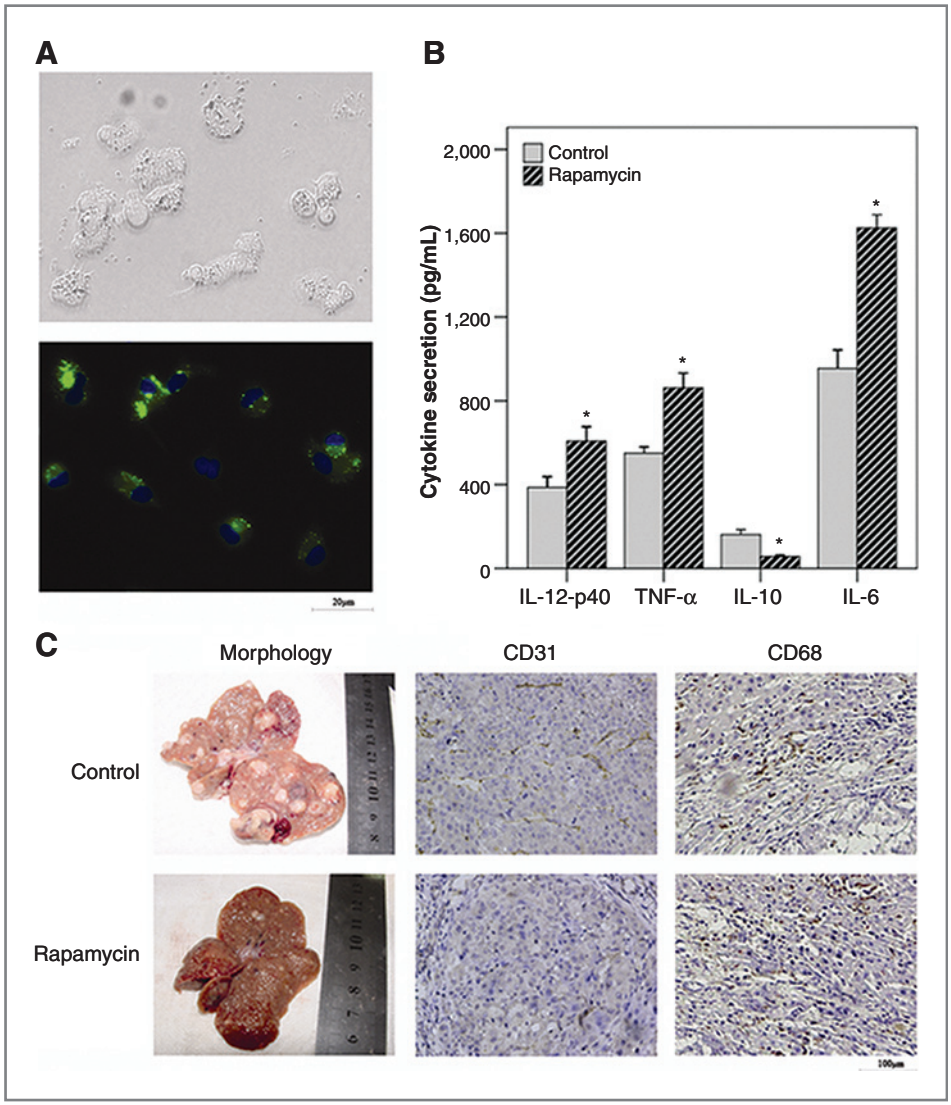

Figure 6. Rapamycin regulated the secretion of cytokines by Kupffer cells from rats and prevented the induction of hepatocarcinogenesis by diethylnitrosamine (DEN) in rats. A, the Kupffer cells isolated from the rats were identified by phagocytosis that was mediated by latex particle (top) and by CD68 immunofluorescence (bottom). B, the production of IL-12-p40, TNF-α, IL-10, and IL-6 by Kupffer cells with different treatment. Data represent mean ± SD. *, a significant difference compared with the control group. C, representative images for rat livers from the rats treated with the control and with rapamycin after DEN treatment. Gross liver appearance are shown on the left; immunohistochemistry examined the expression of CD31 to detect angiogenesis and CD68 to detect Kupffer cells are shown on the right.

had antiangiogenic effects and reduced the release of proangiogenic cytokines (Supplementary Fig. S8A and S8B).

Because STAT proteins regulate cytokine-dependent inflammation and immunity, they are central in determining whether cancer is promoted or inhibited by immune responses (30). The activation of STAT3 mediates such cancer-promoting properties as neoangiogenesis in macrophages (31, 32) and secretion of IL-10 and IL-12 in TAMs (18, 24). We also found that inhibiting STAT3 mediated the upregulation of IL-12 and the downregulation of IL-10 in macrophages, resulting in neoangiogenesis and inhibited tumor growth. The important role of macrophages in this process was shown by the reduced antitumor effects of NSC 74859 when monocytes were depleted. Our results agreed with previous work showing that NSC 74859 inhibits tumor growth more *in vivo* than *in vitro* (33). Our study agreed with the finding of previous studies that STAT3 was the downstream target of mTOR in macrophages and in many other cell types (12, 21). We also found that treatment with NSC 74859 blocked TSC2 siRNA–induced blood vessel formation, indicating that STAT3 was necessary for mTOR-induced angiogenesis. The secretion of cytokines regulated by inhibiting mTOR also involves NK-κB, which regulates IL-12-p40. Inhibiting mTOR led to activation of NK-κB, which augmented the secretion of IL-12-p40, whereas inhibiting STAT3 only impaired the secretion of IL-10 (12). However, this study found that when mTOR was inhibited, STAT3 decreased the secretion of both IL-12-p40 and IL-10. Thus, STAT3 mediates the effects of mTOR in macrophage-induced neoangiogenesis, potentially providing us new insights into innate immune responses and new targets for cancer therapy.

We also found that rapamycin affects Kupffer cells by enhancing IL-12 and inhibiting IL-10 production, indicating that the mTOR pathway is involved in the function of Kupffer cells. Rapamycin reduced the angiogenesis and growth of tumors that were induced by diethylnitrosamine in rats. Additional experiments are required to further investigate that how rapamycin affects tumor formation in the liver.

Published OnlineFirst January 27, 2012; DOI: 10.1158/0008-5472.CAN-11-2684

In summary, we have identified a critical role of the TSC2–mTOR pathway in regulating angiogenesis that is induced by phagocytic cells. When mTOR was activated in monocytes by knocking down TSC2 with siRNA, STAT3 was activated and IL-10 increased while IL-12 decreased in a manner similar to TAM secretion and resulted in neoangiogenesis *in vivo*. Conversely, inhibiting mTOR had a reciprocal effect. These findings suggest that inhibiting TSC2–mTOR–STAT3 in the innate immune response may be a novel and effective therapeutic avenue.

Disclosure of Potential Conflicts of Interest

No potential conflicts of interests were disclosed.

Acknowledgments

Kathy Boltz of MedCom Asia provided professional English language assistance for the manuscript.

Grant Support

This study was supported by grants from the National Natural Science Funds for Distinguished Young Scholar (No. 30925033), the National Natural Science Fund of China (Nos. 30801101 and 81171884), and The Innovation and High-Level Talent Training Program of Department of Health of Zhejiang.

The costs of publication of this article were defrayed in part by the payment of page charges. This article must therefore be hereby marked *advertisement* in accordance with 18 U.S.C. Section 1734 solely to indicate this fact.

Received August 9, 2011; revised January 18, 2012; accepted January 20, 2012; published OnlineFirst January 27, 2012.

References

1. Mantovani A, Allavena P, Sica A, Balkwill F. Cancer-related inflammation. Nature 2008;454:436–44.
2. Berasain C, Castillo J, Perugorria MJ, Latasa MU, Prieto J, Avila MA. Inflammation and liver cancer: new molecular links. Ann N Y Acad Sci 2009;1155:206–21.
3. Mantovani A, Sozzani S, Locati M, Allavena P, Sica A. Macrophage polarization: tumor-associated macrophages as a paradigm for polarized M2 mononuclear phagocytes. Trends Immunol 2002;23:549–55.
4. Murdoch C, Muthana M, Coffelt SB, Lewis CE. The role of myeloid cells in the promotion of tumour angiogenesis. Nat Rev Cancer 2008;8:618–31.
5. Leek RD, Lewis CE, Whitehouse R, Greenall M, Clarke J, Harris AL. Association of macrophage infiltration with angiogenesis and prognosis in invasive breast carcinoma. Cancer Res 1996;56:4625–9.
6. Gazzaniga S, Bravo AI, Guglielmotti A, van Rooijen N, Maschi F, Vecchi A, et al. Targeting tumor-associated macrophages and inhibition of MCP-1 reduce angiogenesis and tumor growth in a human melanoma xenograft. J Invest Dermatol 2007;127:2031–41.
7. Lin EY, Li JF, Gnatovskiy L, Deng Y, Zhu L, Grzesik DA, et al. Macrophages regulate the angiogenic switch in a mouse model of breast cancer. Cancer Res 2006;66:11238–46.
8. Kimura YN, Watari K, Fotovati A, Hosoi F, Yasumoto K, Izumi H, et al. Inflammatory stimuli from macrophages and cancer cells synergistically promote tumor growth and angiogenesis. Cancer Sci 2007;98:2009–18.
9. Laplante M, Sabatini DM. mTOR signaling at a glance. J Cell Sci 2009;122:3589–94.
10. Hay N, Sonenberg N. Upstream and downstream of mTOR. Genes Dev 2004;18:1926–45.
11. Inoki K, Li Y, Zhu T, Wu J, Guan KL. TSC2 is phosphorylated and inhibited by Akt and suppresses mTOR signalling. Nat Cell Biol 2002;4:648–57.
12. Weichhart T, Costantino G, Poglitsch M, Rosner M, Zeyda M, Stuhlmeier KM, et al. The TSC-mTOR signaling pathway regulates the innate inflammatory response. Immunity 2008;29:565–77.
13. Schmitz F, Heit A, Dreher S, Eisenacher K, Mages J, Haas T, et al. Mammalian target of rapamycin (mTOR) orchestrates the defense program of innate immune cells. Eur J Immunol 2008;38:2981–92.
14. Saemann MD, Haidinger M, Hecking M, Horl WH, Weichhart T. The multifunctional role of mTOR in innate immunity: implications for transplant immunity. Am J Transplant 2009;9:2655–61.
15. Yu H, Kortylewski M, Pardoll D. Crosstalk between cancer and immune cells: role of STAT3 in the tumour microenvironment. Nat Rev Immunol 2007;7:41–51.
16. Cheng F, Wang HW, Cuenca A, Huang M, Ghansah T, Brayer J, et al. A critical role for Stat3 signaling in immune tolerance. Immunity 2003;19:425–36.
17. Hasita H, Komohara Y, Okabe H, Masuda T, Ohnishi K, Lei XF, et al. Significance of alternatively activated macrophages in patients with intrahepatic cholangiocarcinoma. Cancer Sci 2010;101:1913–9.
18. Kortylewski M, Xin H, Kujawski M, Lee H, Liu Y, Harris T, et al. Regulation of the IL-23 and IL-12 balance by Stat3 signaling in the tumor microenvironment. Cancer Cell 2009;15:114–23.
19. Sica A, Bronte V. Altered macrophage differentiation and immune dysfunction in tumor development. J Clin Invest 2007;117:1155–66.
20. Niu G, Heller R, Catlett-Falcone R, Coppola D, Jaroszeski M, Dalton W, et al. Gene therapy with dominant-negative Stat3 suppresses growth of the murine melanoma B16 tumor *in vivo*. Cancer Res 1999;59:5059–63.
21. Ma J, Meng Y, Kwiatkowski DJ, Chen X, Peng H, Sun Q, et al. Mammalian target of rapamycin regulates murine and human cell differentiation through STAT3/p63/Jagged/Notch cascade. J Clin Invest 2010;120:103–14.
22. Guba M, von Breitenbuch P, Steinbauer M, Koehl G, Flegel S, Hornung M, et al. Rapamycin inhibits primary and metastatic tumor growth by antiangiogenesis: involvement of vascular endothelial growth factor. Nat Med 2002;8:128–35.
23. Semela D, Piguet AC, Kolev M, Schmitter K, Hlushchuk R, Djonov V, et al. Vascular remodeling and antitumoral effects of mTOR inhibition in a rat model of hepatocellular carcinoma. J Hepatol 2007;46:840–8.
24. Chiang GG, Abraham RT. Phosphorylation of mammalian target of rapamycin (mTOR) at Ser-2448 is mediated by p70S6 kinase. J Biol Chem 2005;280:25485–90.
25. Siddiquee K, Zhang S, Guida WC, Blaskovich MA, Greedy B, Lawrence HR, et al. Selective chemical probe inhibitor of Stat3, identified through structure-based virtual screening, induces antitumor activity. Proc Natl Acad Sci U S A 2007;104:7391–6.
26. Diagaradjane P, Deorukhkar A, Gelovani JG, Maru DM, Krishnan S. Gadolinium chloride augments tumor-specific imaging of targeted quantum dots *in vivo*. ACS Nano 2010;4:4131–41.
27. Hardonk MJ, Dijkhuis FW, Hulstaert CE, Koudstaal J. Heterogeneity of rat liver and spleen macrophages in gadolinium chloride-induced elimination and repopulation. J Leukoc Biol 1992;52:296–302.
28. Saccani A, Schioppa T, Porta C, Biswas SK, Nebuloni M, Vago L, et al. p50 nuclear factor-kappaB overexpression in tumor-associated macrophages inhibits M1 inflammatory responses and antitumor resistance. Cancer Res 2006;66:11432–40.
29. Hagemann T, Lawrence T, McNeish I, Charles KA, Kulbe H, Thompson RG, et al. "Re-educating" tumor-associated macrophages by targeting NF-kappaB. J Exp Med 2008;205:1261–8.
30. Yu H, Pardoll D, Jove R. STATs in cancer inflammation and immunity: a leading role for STAT3. Nat Rev Cancer 2009;9:798–809.
31. Kujawski M, Kortylewski M, Lee H, Herrmann A, Kay H, Yu H. Stat3 mediates myeloid cell-dependent tumor angiogenesis in mice. J Clin Invest 2008;118:3367–77.
32. Matsukawa A, Kudo S, Maeda T, Numata K, Watanabe H, Takeda K, et al. Stat3 in resident macrophages as a repressor protein of inflammatory response. J Immunol 2005;175:3354–9.
33. Lin L, Amin R, Gallicano GI, Glasgow E, Jogunoori W, Jessup JM, et al. The STAT3 inhibitor NSC 74859 is effective in hepatocellular cancers with disrupted TGF-beta signaling. Oncogene 2009;28:961–72.

Published OnlineFirst January 27, 2012; DOI: 10.1158/0008-5472.CAN-11-2684

Cancer Research
The Journal of Cancer Research (1916–1930) | The American Journal of Cancer (1931–1940)

AACR American Association for Cancer Research

Macrophage-Induced Tumor Angiogenesis Is Regulated by the TSC2–mTOR Pathway

Wei Chen, Tao Ma, Xu-ning Shen, et al.

Cancer Res Published OnlineFirst January 27, 2012.